Available online at www.sciencedirect.com
SCIENCE DIRECT®
Intermetallics 12 (2004) 1285–1292
Intermetallics
www.elsevier.com/locate/intermet

# Infrared brazing of $Ti_{50}Ni_{50}$ shape memory alloy using pure Cu and Ti–15Cu–15Ni foils

T.Y. Yang[a], R.K. Shiue[b], S.K. Wu[c,*]

[a]Department of Mechanical Engineering, Kuang Wu Institute of Technology, Taipei 112, Taiwan, ROC
[b]Department of Materials Science and Engineering, National Dong Hwa University, Hualien 974, Taiwan, ROC
[c]Department of Materials Science and Engineering, College of Engineering, National Taiwan University, 1 Roosevelt Road Sec 4, Taipei 106, Taiwan, ROC

Received 1 July 2003; accepted 3 March 2004
Available online 20 May 2004

**Abstract**

Infrared brazing of $Ti_{50}Ni_{50}$ using two brazing filler metals was investigated in the study. Three phases, including Cu-rich, CuNiTi (Δ) and Ti(Ni,Cu), were observed in the $Ti_{50}Ni_{50}$/Cu/$Ti_{50}Ni_{50}$ joint after brazing at 1150 °C. The Cu-rich phase was rapidly consumed in the first 10 s of brazing, and the eutectic mixture of CuNiTi and Ti(Ni,Cu) phases were subsequently observed in the joint. Samples brazed for longer time resulted in less CuNiTi and more Ti(Ni,Cu) phases in the joint. The existence of CuNiTi phase deteriorated the shape memory effect of the joint, but Ti(Ni,Cu) could still preserve shape memory behavior even alloyed with a large number of Cu. Therefore, higher shape recovery ratio was observed for specimens brazed for a longer time period. Extensive presence of $Ti_2$(Ni,Cu) phase was observed in $Ti_{50}Ni_{50}$/Ticuni®/$Ti_{50}Ni_{50}$ joint upon brazing the specimens up to 1150 °C. The bending test could not be performed due to the inherent brittleness of $Ti_2$(Ni,Cu) matrix. Moreover, the stable $Ti_2$(Ni,Cu) phase was difficult to be removed completely by increasing either brazing time and/or temperature.


*Keywords:* A. Intermetallics, miscellaneous; B. Shape-memory effects; C. Joining; D. Microstructure; E. Phase diagram

## 1. Introduction

The importance of TiNi-based shape memory alloys (SMAs) is increasing due to their superior behavior in shape memory effect, superelasticity, and high corrosion resistance compared with many other SMAs [1–6]. The maturity of various manufacturing processes plays an important role in the applications of TiNi-based SMAs, and rolling, drawing as well as joining have been extensively studied [7–12].

Brazing is an economical fabrication method of complex assemblies among all joining methods [13]. Although there is no melting of the base metal during brazing, the heating can still affect the properties of the materials being joined [13]. It will be highly preferred that minimum heating is introduced during brazing in order to avoid deterioration of the base metal. The rapid infrared joining technique has been originally developed at the University of Cincinnati for high temperature materials [14]. Infrared brazing is a novel technique featured with rapid thermal cycle in comparison with the traditional furnace brazing [15]. With the aid of infrared energy generated by heating a tungsten filament in a quartz tube, the infrared furnace can provide rapid heating rate up to 3000 °C/min [15]. Therefore, the infrared brazing is highly suitable for studying the mechanism of early-stage reaction kinetics in the joint, and many reports are already available in literatures [16–19]. Infrared brazing has become an important method in studying the microstructural evolution of the brazed joint.

The primary challenge in brazing TiNi-based SMAs is to preserve its shape memory characteristics across the joined interface. Conventional furnace brazing with slow heating rates is probably not suitable in bonding TiNi-based SMAs, because the base metal experiences elevated temperatures for a long time. The reaction of Ti with other elements at elevated temperatures may deteriorate many featured properties of TiNi-based SMAs. Consequently, the investigation of brazing TiNi SMA is very limited [11].

* Corresponding author. Tel.: +886-2-2363-7846; fax: +886-2-2363-4562.
*E-mail address:* skw@ccms.ntu.edu.tw (S.K. Wu).

0966-9795/$ - see front matter © 2004 Elsevier Ltd. All rights reserved.
doi:10.1016/j.intermet.2004.03.020

It is reported that Ni atoms can be replaced by a large number of Cu atoms in $Ti_{50}Ni_{50}$ alloy and $Ti_{50}Ni_{50-x}Cu_x$ ($x \leqq 30$ wt.%) SMAs can still exhibit shape memory behavior [20,21]. Consequently, both pure Cu and Ti–15Cu–15Ni foils are selected as brazing filler metals in joining $Ti_{50}Ni_{50}$ SMA. It is well known that the properties of the bonding interface between filler metal and base metal are strongly related to the interfacial microstructure. The morphology, quantity and species of the phases at the interface play crucial roles in evaluating the brazed joint. The main purpose of this study is aimed to infrared brazing $Ti_{50}Ni_{50}$ SMA using two filler metals, pure Cu and Ti–15Cu–15Ni, respectively. With the aid of fast infrared heating rate, the early-stage of microstructural evolution in the joint will be studied extensively. The shape recovery character of an infrared-joined $Ti_{50}Ni_{50}$ SMA is also discussed.

## 2. Experimental procedures

$Ti_{50}Ni_{50}$ in atomic percent was used as the base metal in this study. The master alloy was prepared by vacuum arc remelting using high-purity pellets under protective argon atmosphere. The TiNi ingot was firstly cut into approximate 10 mm × 5 mm × 1 mm specimens. Brazed surfaces of each TiNi specimen were polished by a SiC paper of 600 grit, and subsequently cleaned well in an ultrasonic bath prior to infrared brazing. Pure copper foil and Ticuni® foil of thickness 25 μm as well as 50 μm were used as the brazing filler metals. Ticuni® foil is a commercial product of Wesgo company, and its chemical composition in weight percent is 70Ti–15Cu–15Ni. Ticuni® is a clad-laminated brazing filler metal [22]. It has an inner $Cu_{50}Ni_{50}$ (wt.%) alloy layer and two pure outer Ti layers. The solidus and liquidus temperatures of Ticuni® foil are 910 and 960 °C, respectively.

The brazing filler foil was sandwiched by two pieces of $Ti_{50}Ni_{50}$ base metal. To enhance infrared absorption of the brazed specimen, all specimens were clamped between two graphite plates, and a thermocouple was kept in contact with the specimen as shown in Fig. 1 to measure the temperature. An ULVAC SINKO-RIKO RHL-P610C infrared furnace with an Ar flow rate of 200 $cm^3$/min was used throughout the experiment. Table 1 summaries all process variables used in this study. The specimen was cut by a low speed diamond saw. A standard metallographic procedure was applied to the specimen before the microstructural observation. Their cross-sections were first ground by SiC papers, and subsequently polished by 0.3 μm alumina powder. Kroll's reagent with 2 ml HF, 4 ml $HNO_3$ and 100 ml $H_2O$ was selected as an etching solution. The etched cross-sections of the brazed specimens were examined using a Philips XL30 scanning electron microscope (SEM) with energy dispersive X-ray spectroscopy (EDS). Quantitative chemical analysis was also performed using a JEOL JXA-8600SX electron probe microanalyzer (EPMA) equipped with a wavelength dispersive spectrometer (WDS) operated at 15 kV with a probe current of 100 nA.

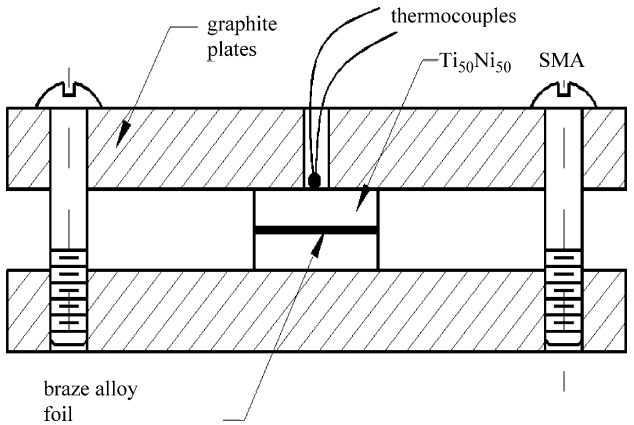


Fig. 1. The schematic diagram showing geometry of graphite fixture used in the test.

The shape memory effect (SME) was measured by the bending test to evaluate the shape recovery ratio of infrared brazed joint [23]. Fig. 2 displays a schematic diagram of the bending test. The initially flat brazed $Ti_{50}Ni_{50}$/Cu/$Ti_{50}Ni_{50}$ and $Ti_{50}Ni_{50}$/Ticuni®/$Ti_{50}Ni_{50}$ specimens were machined into a size of approximately 20 mm × 5 mm × 0.5 mm. Then, it was bent into an angle $\theta_i$ at the temperature of 77 K (liquid nitrogen). After the temperature was raised to various temperatures of up to 130 °C, $\theta_i$ was recovered to $\theta_f$, which was temperature dependent. The shape recovery ratio of the joint was determined by $(\theta_i - \theta_f)/\theta_i$. The detailed measurement of the shape-recovery characteristics has been presented elsewhere [23]. A pure $Ti_{50}Ni_{50}$ specimen with the same dimension of the above infrared brazed sample was also tested for the purpose of comparison.

Table 1
Process variables used in infrared brazing

| Temperature (°C) | $Ti_{50}Ni_{50}$/Cu/$Ti_{50}Ni_{50}$ (s) | $Ti_{50}Ni_{50}$/Ticuni®/$Ti_{50}Ni_{50}$ (s) |
|---|---|---|
| 960 | – | 12 |
| 960 | – | 30 |
| 960 | – | 120 |
| 960 | – | 300 |
| 1000 | – | 30 |
| 1050 | – | 30 |
| 1100 | – | 30 |
| 1150 | 2 | – |
| 1150 | 10 | – |
| 1150 | 30 | 30 |
| 1150 | 60 | – |
| 1150 | 300 | – |

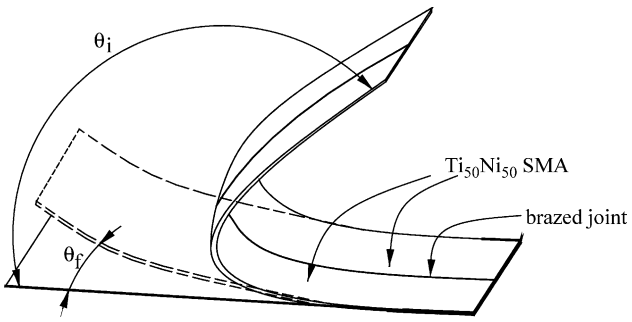


Fig. 2. The schematic diagram of the bending test.

## 3. Results and discussion

### 3.1. Infrared brazing of $Ti_{50}Ni_{50}$/Cu/$Ti_{50}Ni_{50}$ Joint

The heating of substrate may result in changes of its properties, particularly if the alloy is heated above its annealing temperatures. Where mechanical properties are obtained by heat treatment, e.g. quench and temper, they may be altered by the brazing operation. In contrast, the alloy in the annealed condition will generally experience no appreciable change due to brazing [24]. It is expected that brazing has little effect on the mechanical properties of TiNi substrate. Additionally, one of the significant

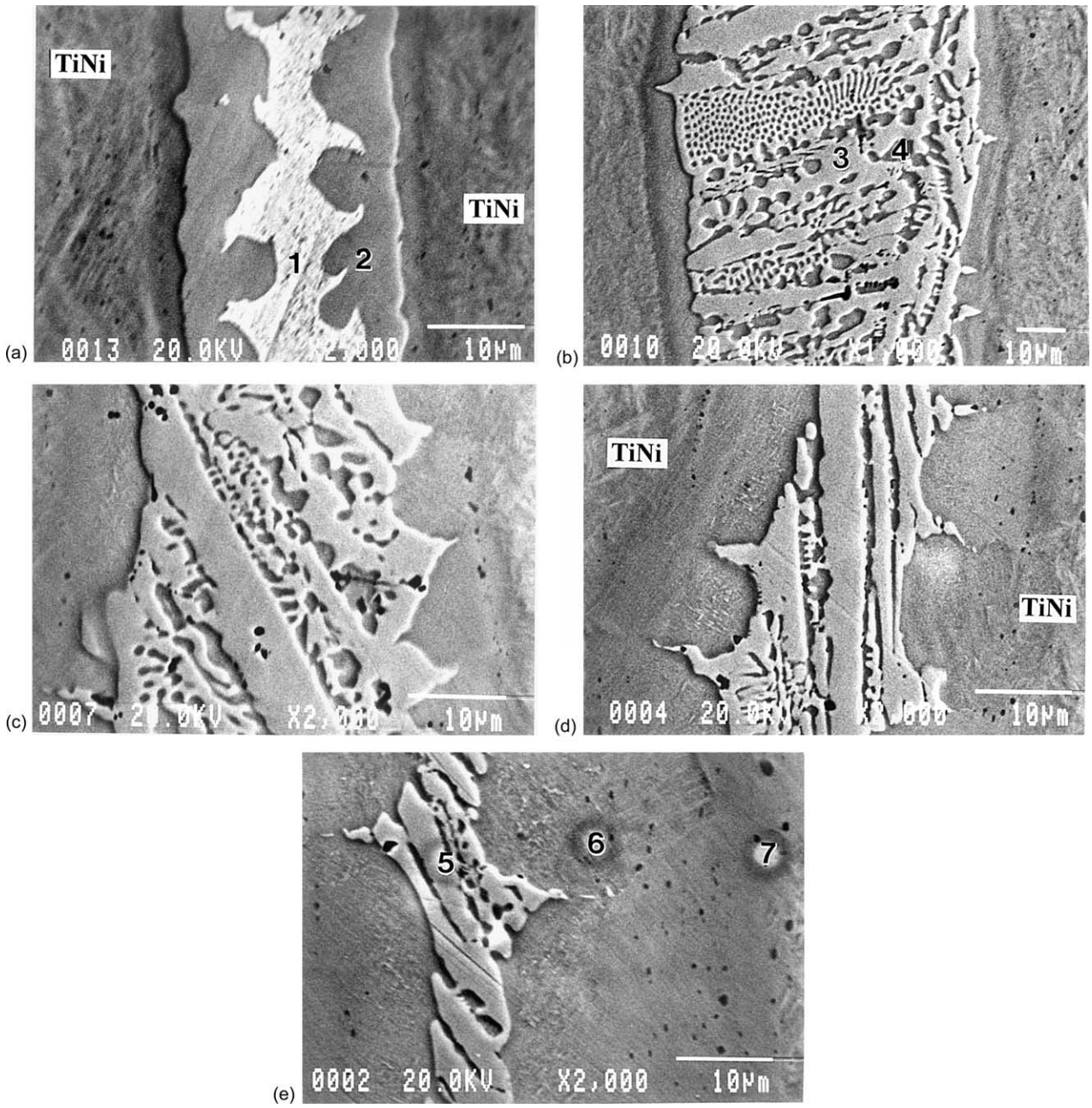


Fig. 3. The BEIs of the interface infrared brazed at 1150 °C for (a) 2 s, (b) 10 s, (c) 30 s, (d) 60 s, and (e) 300 s.

Table 2
Chemical analyses of the selected areas in Fig. 3

| No. | Composition (at.%) | Remarks |
|---|---|---|
| 1 | 4.7Ti–2.6Ni–92.7Cu | Cu-rich phase |
| 2 | 34.8Ti–35.5Ni–29.7Cu | CuNiTi (Δ) phase |
| 3 | 34.8Ti–38.1Ni–27.0Cu | CuNiTi (Δ) phase |
| 4 | 48.2Ti–40.8Ni–11.0Cu | Ti (Ni,Cu) phase |
| 5 | 37.4Ti–39.0Ni–23.5Cu | CuNiTi (Δ) phase |
| 6 | 48.2Ti–44.1Ni–7.7Cu | Ti (Ni,Cu) phase |
| 7 | 50.6Ti–48.2Ni–1.2Cu | Ti (Ni,Cu) phase |

base metal interactions which have been used in determining the behavior of brazed joint is alloying. The extent of interaction varies greatly depending on the compositions of the base metal, the brazing filler metal and thermal cycle [24]. A short thermal cycle can usually minimize the alloying effect during brazing. Compared with the traditional furnace brazing, infrared brazing is featured with a very rapid thermal cycle, so higher infrared brazing temperature will do less damage to the base metal. However, high brazing temperature can greatly speed up the microstructural evolution of the brazed joint in the study.

The melting point of pure Cu is 1084.9 °C, so 1150 °C was the chosen as the brazing temperature throughout the experiment. Fig. 3 displays backscattered electron images (BEIs) of the interface infrared-brazed specimen at 1150 °C for 2, 10, 30, 60 and 300 s. Numbers 1–7 shown in the figure are the chemical analyses of the selected areas, and the results are listed in Table 2. According to Table 2, there are three phases observed in the joint, including: Cu-rich phase, CuNiTi (Δ) phase and Ti(Ni,Cu) phase [25]. Residual Cu can be initially found in the joint, but it is completely consumed in 10 s as shown in Fig. 3(a) and (b). In Fig. 3(a), the central Cu-rich phase (marked by 1) is alloyed with minor Ti and Ni, and a CuNiTi phase (marked by 2) is intermediated between the Cu-rich phase and $Ti_{50}Ni_{50}$ base metal. The dissolution of $Ti_{50}Ni_{50}$ base metal into molten Cu-rich braze results in the formation of CuNiTi phase. The ternary CuNiTi (Δ) intermetallic compound with a stoichiometry $Cu_{30}Ni_{36.5}Ti_{33.5}$ has been reported in the literature [25]. The microstructure displayed in Fig. 3(b) exhibits the eutectic structure of CuNiTi and Ti(Ni,Cu). It was reported that high solubility of Cu was found in $Ti_{50}Ni_{50}$, with Ni being replaced by Cu [20,21].

Fig. 4 shows the isothermal section of Cu–Ni–Ti system at 800 °C in atomic percent [25]. According to Fig. 4, TiNi has a huge solubility for Cu, and it is consistent with our experimental result. There are two major regions between TiNi and Cu in Fig. 4, including a region mixed with

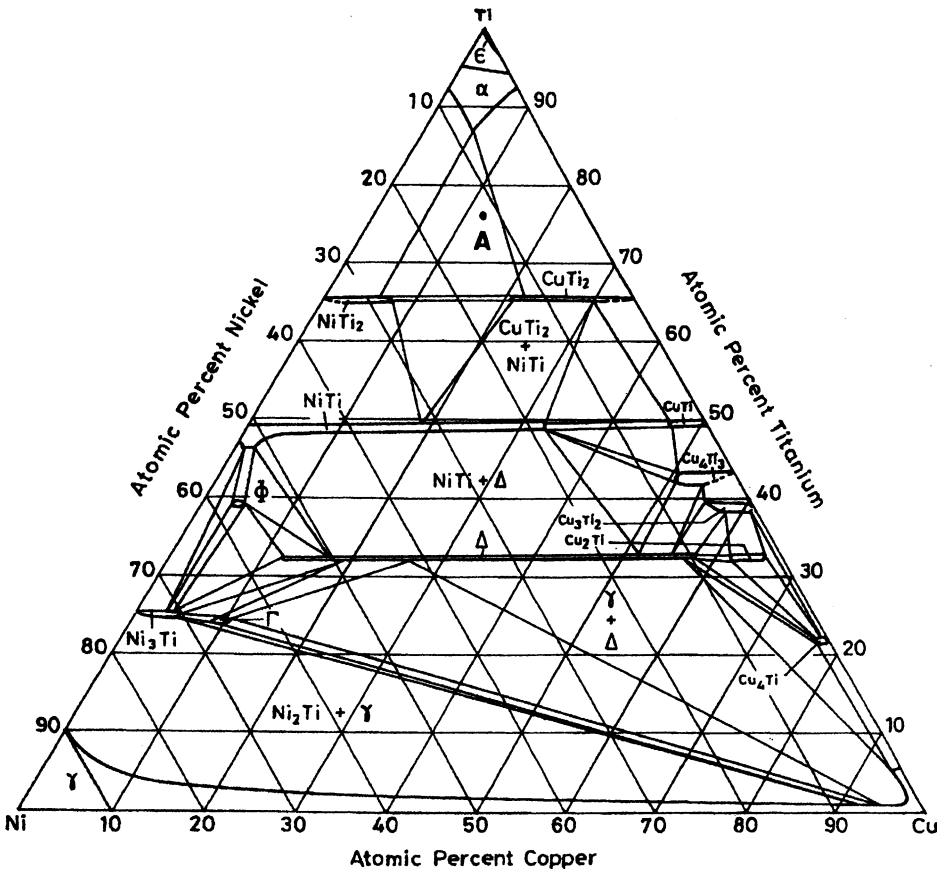


Fig. 4. The isothermal section in the Cu–Ni–Ti system at 800 °C in atomic percent [25].

Ti(Ni,Cu) and CuNiTi (NiTi + Δ), and a region mixed with CuNiTi and Cu-rich phase (Δ + γ). The dissolution $Ti_{50}Ni_{50}$ substrate into the molten braze is strongly related to the final microstructure of the joint. With the increment of brazing time, both the diffusion of Cu atoms into $Ti_{50}Ni_{50}$ substrate and Ni atoms into the braze are greatly enhanced. The formation of CuNiTi phase in the braze results in the disappearance of Cu-rich phase in the joint, so the eutectic Ti(Ni,Cu) and CuNiTi phase, instead of eutectic CuNiTi and Cu-rich phase, is observed in the experiment. Additionally, the amount of CuNiTi phase in the joint is gradually decreased with the increment of brazing time, because the TiNi substrate has a huge solubility of Cu. The consumption of Cu from the CuNiTi phase cause shrinkage of CuNiTi in the infrared brazed joint as illustrated in Fig. 3(c)–(e). According to the experimental observations, it is expected that CuNiTi phase can be completely dissolved into $Ti_{50}Ni_{50}$ substrate if the brazing time is long enough.

The infrared brazing $Ti_{50}Ni_{50}$ using pure Cu consists of several major stages, including: melting of the braze alloy (Cu), dissolution of the $Ti_{50}Ni_{50}$ into the Cu-rich melt, saturation of the melt, isothermal solidification of the molten braze alloy and homogenization of the brazed joint through diffusion of the solute atoms into the base metal [26]. It is similar to the process of transient liquid phase bonding (TLPB) [26–28]. The melting of Cu during infrared brazing is very rapid as demonstrated in Fig. 3(a). In contrast, the isothermal solidification and homogenization are not completed during infrared joining. Blue proposes an estimation of the time for isothermal solidification at various specified joining temperatures [26]. However, there is no further calculation in this research due to insufficient diffusion data of Cu and Ti atoms in $Ti_{50}Ni_{50}$ substrate. Accordingly, it needs further study in the future.

Table 3 summaries the result of the bending test. The shape recovery ratio of the original $Ti_{50}Ni_{50}$ strip is 95% at 80 °C, and it increases to 99% as the specimen heated to 130 °C. Higher recovery ratio can be obtained for all specimens heated to a higher temperature. According to Table 3, the recovery ratio of the specimen brazed for 300 s is better than that of specimens brazed for 60 s. There are two different thickness of the Cu foils used in the test, including 50 and 25 μm. Both thicknesses of the Cu fillers demonstrate similar tendency of the test.

Table 3
Shape memory recovery of $Ti_{50}Ni_{50}$/Cu/$Ti_{50}Ni_{50}$ joint

| Specimen | Shape recovery at 80 °C (%) | Shape recovery at 130 °C (%) |
|---|---|---|
| 50 μm Cu foil, 60 s | 60 | 83 |
| | 53 | 81 |
| 50 μm Cu foil,300 s | 87 | >99 |
| | 84 | >99 |
| 25 μm Cu foil, 60 s | 64 | 81 |
| 25 μm Cu foil,300 s | 98 | >99 |
| $Ti_{50}Ni_{50}$ Base metal | 95 | >99 |

According to the aforementioned result, specimens brazed for longer time result in less CuNiTi phase and more Ti(Ni,Cu) phase in the joint. It is reasonable to conclude that the existence of CuNiTi phase deteriorates the shape memory effect of the joint. Moreover, Ti(Ni,Cu) still preserves the shape memory behavior even though it is alloyed with Cu [20,21]. The amount of CuNiTi phase is greatly decreased in the joint as the brazing time is increased. Therefore, it is expected that

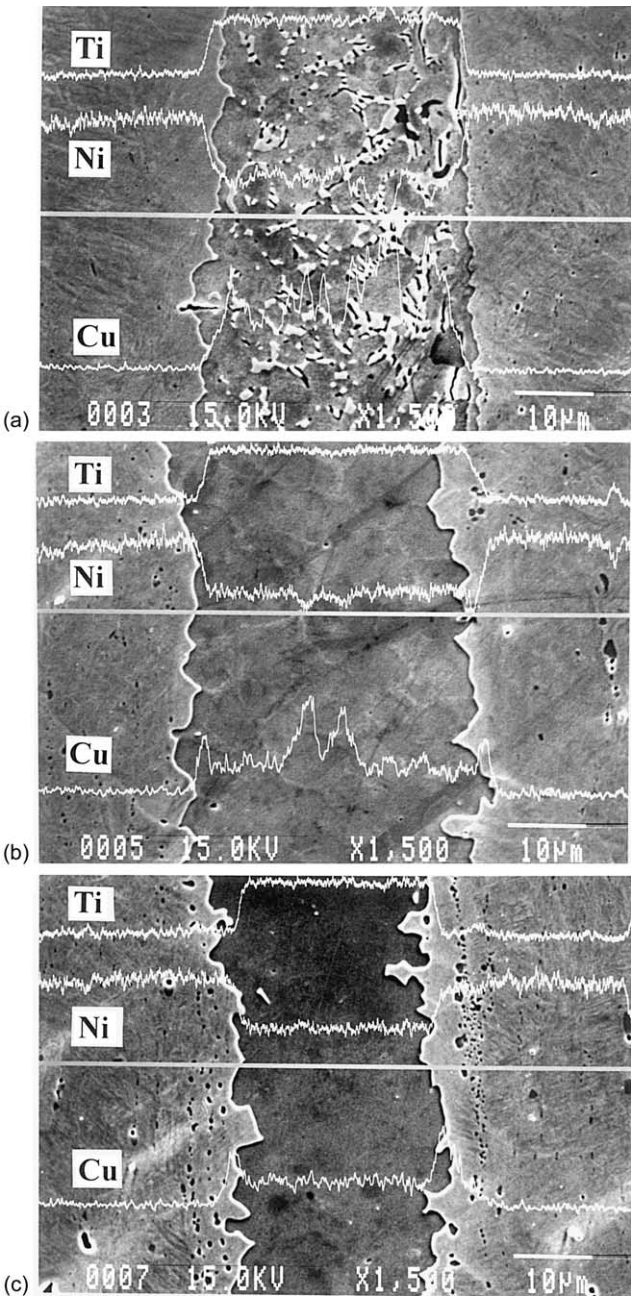


Fig. 5. The SEIs and EPMA line scan profiles of the interface infrared brazed at 960 °C for (a) 12 s, (b) 120 s, and (c) 300 s.

higher shape recovery ratio can be obtained for specimens brazed for a longer time period.

Specimens after bending test were subsequently examined by an SEM. It was confirmed that there was no cracks observed in the $Ti_{50}Ni_{50}$/Cu/$Ti_{50}Ni_{50}$ joint. Consequently, the use of pure Cu in brazing $Ti_{50}Ni_{50}$ has the potential in engineering applications.

### 3.2. Infrared brazing of $Ti_{50}Ni_{50}$/Ticuni®/$Ti_{50}Ni_{50}$ Joint

Fig. 5 displays the secondary electron images (SEIs) and EPMA line scan profiles of the interface infrared brazed at 960 °C for 12, 120 and 300 s. The brazed joint initially contains two phases, the matrix and the angular phase. Upon increasing the brazing time, only the matrix phase is left in the joint. Meanwhile, the line scan profiles demonstrate that the chemical composition of the braze becomes homogeneous upon increasing the brazing time. Chemical analysis using EPMA or EDS is necessary in order to further quantify these phases.

Fig. 6 displays SEM image and EDS chemical analyses of the specimen brazed at 960 °C for 30 s. It is noted that no interfacial reaction phase between $Ti_{50}Ni_{50}$ base metal and the braze alloy is observed. According to EDS analyses, the chemical composition of base metal is close to $Ti_{50}Ni_{50}$ as marked by 1 in Fig. 6. The base metal near the interface is alloyed with more Cu (marked by 2 in Fig. 6), and its stoichiometry is close to $Ti_{50}(Ni,Cu)_{50}$. Unlike aforementioned $Ti_{50}Ni_{50}$/Cu/$Ti_{50}Ni_{50}$ bonding, the current brazed joint is primarily comprised of $Ti_2(Ni,Cu)$ phase (marked by 3 in Fig. 6). Meanwhile, the chemical composition of the angular phase in the joint is still close to $Ti_2(Ni,Cu)$ as shown in Fig. 6 (marked by 4). The major difference between the matrix and the angular phase is the copper content in $Ti_2(Ni,Cu)$. The copper content in the matrix is lower than that in the angular phase. The Cu atoms can replace the Ni atoms in $Ti_2Ni$ phase, so $Ti_2(Ni,Cu)$ is formed during brazing.

Both Ti and Cu diffuse from braze alloy into $Ti_{50}Ni_{50}$, and Ni diffuses from $Ti_{50}Ni_{50}$ into braze driven by the concentration gradient of the joined alloys. According to Fig. 4, the isothermal section in the Cu–Ni–Ti system at 800 °C demonstrates that $Ti_2Ni$ phase can dissolve Cu up to 8 at% [25]. Additionally, there is no intermediate phase between $Ti_{50}Ni_{50}$ and $Ti_2Ni$ as displayed in Fig. 4. It is consistent with our experimental observations. The atomic composition of Ti–15Cu–15Ni is 74.8Ti–12.1 Cu–13.1Ni as marked by A in Fig. 4 [25]. Both $Ti_{50}Ni_{50}$ and $Ti_2Ni$ phases can dissolve Cu, so Ti(Ni,Cu) and $Ti_2(Ni,Cu)$ phases are observed in the experiment.

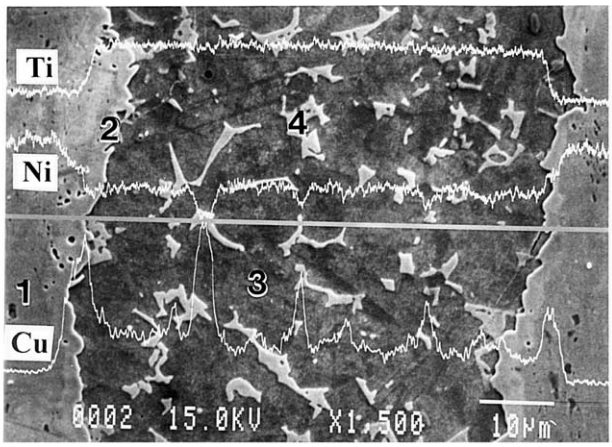


| Element (at%) | 1 | 2 | 3 | 4 |
|---|---|---|---|---|
| Ti | 54.9 | 50.2 | 65.2 | 64.6 |
| Ni | 44.3 | 40.6 | 29.3 | 24.8 |
| Cu | 0.8 | 9.2 | 5.5 | 10.6 |

Fig. 6. The BEI and EDS chemical analyses of the specimen brazed at 960 °C for 30 s.

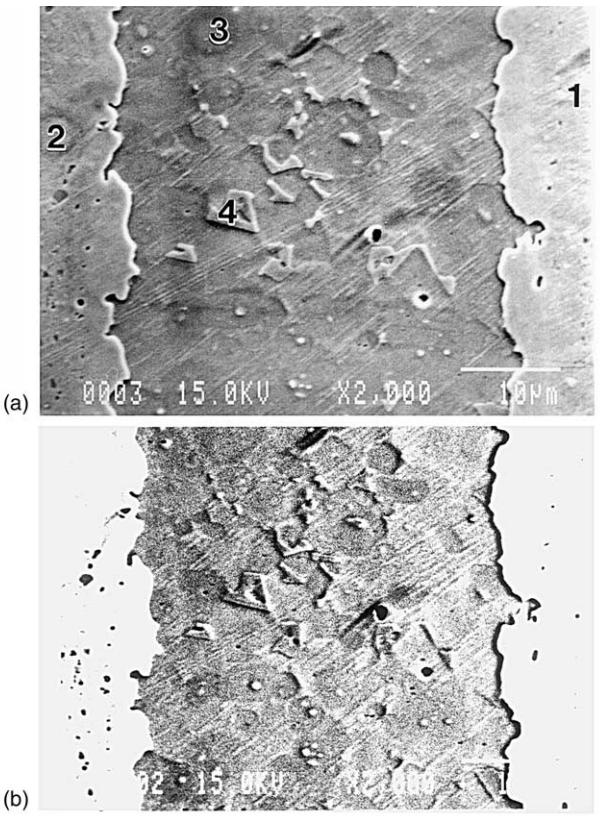


| Element (at%) | 1 | 2 | 3 | 4 |
|---|---|---|---|---|
| Ti | 51.6 | 53.0 | 68.1 | 67.5 |
| Ni | 48.4 | 38.2 | 29.4 | 22.1 |
| Cu | 0.0 | 8.8 | 2.5 | 10.4 |

Fig. 7. The SEM images (a) SEI, (b) BEI, and EPMA chemical analyses of the specimen brazed at 1000 °C for 30 s.

Fig. 7 shows the SEM images and EPMA chemical analyses of the $Ti_{50}Ni_{50}$/Ticuni®/$Ti_{50}Ni_{50}$ joint at 1000 °C for 30 s. The result of EPMA chemical analyses is similar to that brazed at 960 °C for 30 s. Upon increasing the brazing temperature, the amount of angular phase in the joint decreases since the interdiffusion between the molten braze and $Ti_{50}Ni_{50}$ substrate is greatly enhanced at higher brazing temperatures. The consumption of Cu in the molten braze increases at 1000 °C. Consequently, the angular phase with higher Cu content is decreased. Fig. 8 shows the SEM images and EPMA chemical analyses of the $Ti_{50}Ni_{50}$/Ticuni®/$Ti_{50}Ni_{50}$ joint at 1050 °C for 30 s. The angular phase is almost disappeared, and the width of $Ti_2$(Ni,Cu) matrix is further decreased. The depletion of Ti in the braze results in the diminishing of $Ti_2$(Ni,Cu) phase. Similar observation can be found for $Ti_{50}Ni_{50}$/Ticuni®/$Ti_{50}Ni_{50}$ specimens brazed at 1100 °C for 30 s, as displayed in Fig. 9.

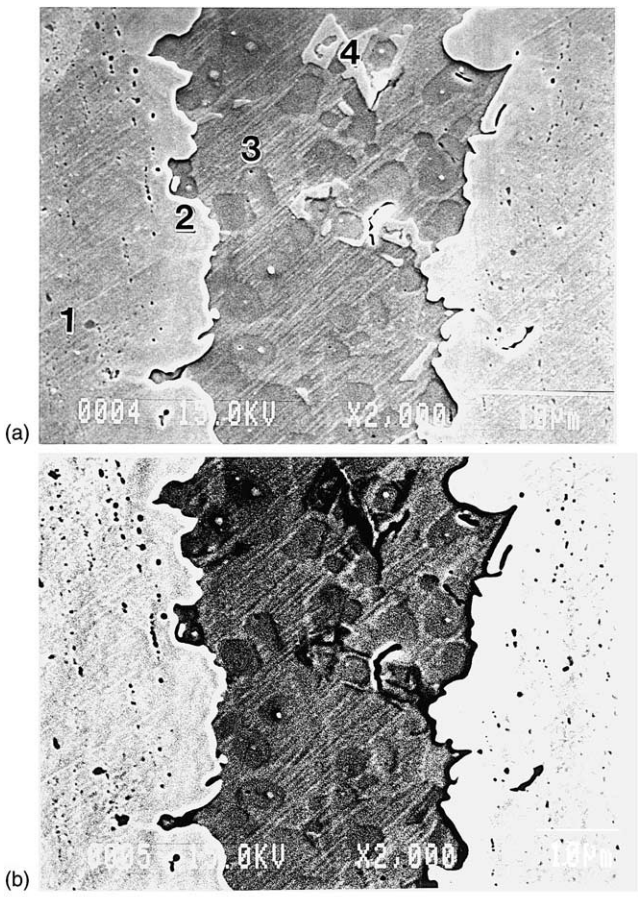


| Element (at%) | 1 | 2 | 3 | 4 |
|---|---|---|---|---|
| Ti | 51.7 | 52.1 | 68.1 | 67.0 |
| Ni | 48.3 | 43.3 | 29.9 | 20.1 |
| Cu | 0.0 | 5.6 | 2.0 | 12.9 |

Fig. 8. The SEM images (a) SEI, (b) BEI, and EPMA chemical analyses of the specimen brazed at 1050 °C for 30 s.

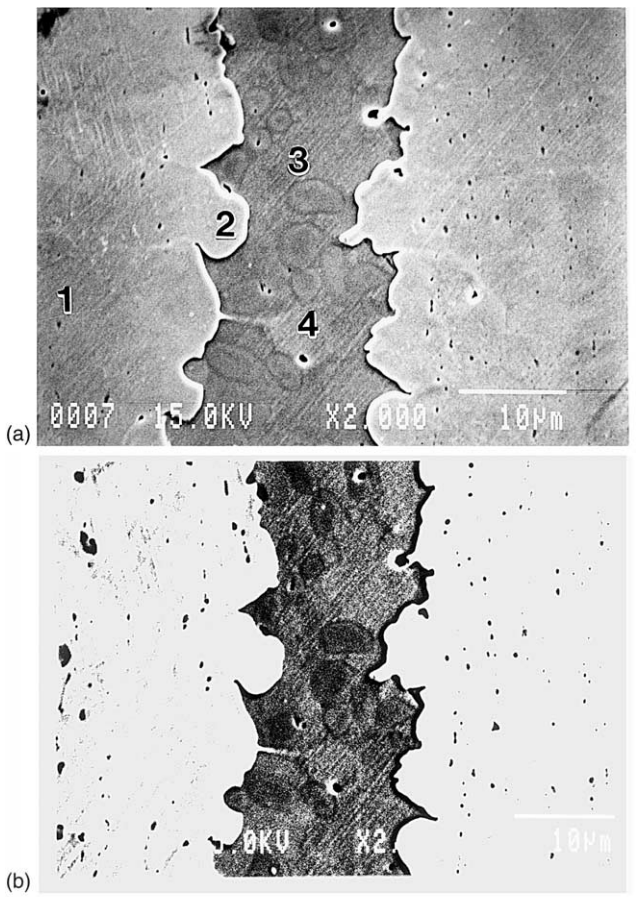


| Element (at%) | 1 | 2 | 3 | 4 |
|---|---|---|---|---|
| Ti | 51.1 | 51.9 | 68.0 | 68.2 |
| Ni | 48.9 | 47.5 | 30.0 | 30.5 |
| Cu | 0.0 | 0.6 | 2.0 | 1.2 |

Fig. 9. The SEM images (a) SEI, (b) BEI and EPMA chemical analyses of the specimen brazed at 1100 °C for 30 s.

The bending test could not be performed due to the inherent brittleness of the infrared brazed joint. $Ti_{50}Ni_{50}$/Ticuni®/$Ti_{50}Ni_{50}$ was broken at the joint after the specimen was bent. The direction of crack propagation was along the braze joint. It was resulted from the extensive presence of brittle $Ti_2$(Ni,Cu) matrix in the joint. In $Ti_{50}Ni_{50}$/Cu/$Ti_{50}Ni_{50}$ bonding, the joint was primarily comprised of eutectic Ti(Ni,Cu) and CuNiTi phase. It was reported that Ti(Ni,Cu) phase still preserved SMA even alloyed with ~30 wt% Cu [20,21]. However, Ti(Ni,Cu) phase was absent from $Ti_{50}Ni_{50}$/Ticuni®/$Ti_{50}Ni_{50}$ joint after infrared brazing. Moreover, $Ti_2$(Ni,Cu) phase was still observed in $Ti_{50}Ni_{50}$/Ticuni®/$Ti_{50}Ni_{50}$ for specimens infrared brazing up to 1150 °C. Consequently, the brittle and stable $Ti_2$(Ni,Cu) phase was difficult to be completely removed by increasing either brazing time or temperature.

## 4. Conclusions

1. Infrared brazing of $Ti_{50}Ni_{50}$/Cu/$Ti_{50}Ni_{50}$ was investigated in the study. Three phases, including Cu-rich, CuNiTi (Δ) and Ti(Ni,Cu), were observed in the joint after infrared brazing at 1150 °C. The Cu-rich phase was rapidly consumed within the first 10 s of brazing. Thereafter, eutectic mixture of CuNiTi and Ti(Ni,Cu) phases was observed in the bond. With the increase of brazing time, the amount of CuNiTi phase decreased due to the consumption of Cu in the joint.
2. The shape recovery ratio of the original $Ti_{50}Ni_{50}$ strip was 95% at 80 °C and 99% at 130 °C in the bending test. The shape recovery ratio of $Ti_{50}Ni_{50}$/Cu/$Ti_{50}Ni_{50}$ joint could reach 99% at 130 °C for the specimen infrared brazed at 1150 °C for 300 s. Samples brazed for longer time resulted in less CuNiTi phase and more Ti(Ni,Cu) phase in the joint. The existence of CuNiTi phase deteriorated the shape memory effect of the joint, but Ti(Ni,Cu) still preserved the shape memory behavior even alloyed with a large number of Cu.
3. Extensive presence of $Ti_2$(Ni,Cu) phase was observed in $Ti_{50}Ni_{50}$/Ticuni®/$Ti_{50}Ni_{50}$ joint for specimens infrared brazed up to 1150 °C for 30 s. The bending test could not be completed due to the inherent brittleness of $Ti_2$(Ni,Cu) matrix in the joint. Moreover, the stable $Ti_2$(Ni,Cu) phase was difficult to be removed by increasing either the brazing temperature or time.

## Acknowledgements

The authors gratefully acknowledge the financial support of this research by the National Science Council (NSC), Republic of China under grant No: NSC 89-2216-E002-002.

## References

[1] Otsuka K, Shimizu K. Inter Metal Rev 1986;31:93.
[2] Miyazaki S, Otsuka K. ISIJ Int 1989;29:353.
[3] Waymam CM. Mater Sci Forum 1989;56–58:1.
[4] Lin HC, Wu SK, Chou TS, Kao HP. Acta Metall 1991;39:2069.
[5] Oshida Y, Miyazaki S. Corrosion Eng 1991;40:1009.
[6] Saburi T. In: Otsuka K, Wayman CM, editors. Shape memory materials. Cambridge: Cambridge University Press; 1998. p. 58.
[7] Miyazaki S, Imai T, Igo Y, Otsuka K. Metall Trans 1986;17A:115.
[8] Liu Y, McCormick PG. Acta Metall Mater 1990;38:1321.
[9] Lin HC, Wu SK. Acta Metall Mater 1994;42:1623.
[10] Wu SK, Lin HC, Yen YC. Mater Sci Eng 1996;215A:113.
[11] Gale WF, Guan Y. J Mater Sci 1997;32:357.
[12] Hsu YT, Wang YR, Wu SK, Chen C. Metall Mater Trans 2001; 32A:569.
[13] Schwartz M. Brazing: for the engineering technologist. New York: Chapman and Hall; 1995. p. 1.
[14] Blue CA, Lin RY. Joining and adhesion of advanced inorganic materials. MRS Symp Proc 1993;314:143.
[15] Shiue RK, Wu SK, O JM, Wang JY. Metall Mater Trans A 2000;31A: 25–7.
[16] Shiue RK, Wu SK, Chen SY. Acta Mater 2003;51:1991.
[17] Shiue RK, Wu SK, Hung CM. Metall Mater Trans A 2002;33A: 1765.
[18] Yang TY, Wu SK, Shiue RK. Intermetallics 2001;9:341.
[19] Lee YL, Shiue RK, Wu SK. Intermetallics 2003;11:187.
[20] Mercier O, Melton KN. Metall Trans 1979;10A:387.
[21] Bricknell RH, Melton KN. Metall Trans 1979;10A:1541.
[22] Hoffman EK, Bird RK, Dicus DL. Welding J 1995;74:378s.
[23] Lin HC, Wu SK. Scripta Metall Mater 1992;26:59.
[24] Schwartz M. Brazing. Metals Park, OH: ASM International; 1987. p. 39.
[25] Gupta KP, Phase diagrams of ternary nickel alloys, Calcutta: Indian Institute of Metals; 1990. p. 258.
[26] Blue CA, Sikka VK, Blue RA, Lin RY. Metall Mater 1996;27A:1.
[27] Tuah-Poku I, Dollar M, Massalski TB. Metall Mater 1988;19A: 675.
[28] MacDonald WD, Eagar TW. Annu Rev Mater Sci 1992;22:23.